

A SIMPLE METHOD FOR MEASURING THE ELECTRON-BEAM MAGNETIZATION*

A. Halavanau^{1,2}, G. Qiang^{3,4}, E. Wisniewski³, G. Ha⁵, J. Power³, P. Piot^{1,2}

¹ Department of Physics and Northern Illinois Center for Accelerator & Detector Development, Northern Illinois University, DeKalb, IL 60115, USA

² Fermi National Accelerator Laboratory, Batavia, IL 60510, USA

³ Argonne Wakefield Accelerator, Argonne National Laboratory, Lemont, IL, 60439, USA

⁴ Accelerator laboratory, Department of Engineering Physics, Tsinghua University, Beijing, China

⁵ POSTECH, Pohang, Kyungbuk, 37673, Korea

Abstract

There are a number of projects that require magnetized beams, such as electron cooling or aiding in “flat” beam transforms. Here we explore a simple technique to characterize the magnetization, observed through the angular momentum of magnetized beams. These beams are produced through photoemission. The generating drive laser first passes through microlens arrays (fly-eye light condensers) to form a transversely modulated pulse incident on the photocathode surface [1]. The resulting charge distribution is then accelerated from the photocathode. We explore the evolution of the pattern via the relative shearing of the beamlets, providing information about the angular momentum. This method is illustrated through numerical simulations and preliminary measurements carried out at the Argonne Wakefield Accelerator (AWA) facility are presented.

CHARACTERIZATION OF THE MAGNETIZED BEAM

When electron beam is born in presence of an axial magnetic field, it forms a “magnetized” beam state. Such beams have a variety of applications in electron cooling and can lead to the formation of beams with asymmetric transverse emittances or “flat” beams [2].

According to Busch’s theorem the total canonical angular momentum (CAM) of a charged particle in axially symmetric magnetic field is conserved and given by [3]:

$$L = \gamma m r^2 \dot{\theta} + \frac{1}{2} e B_z(z) r^2, \quad (1)$$

where (r, θ, z) are cylindrical coordinates.

We now specialize on the case of the Argonne Wakefield Accelerator (AWA) “witness” beamline illustrated in Fig. 1. The beamline includes a L-band RF gun with a Mg photocathode on its back plate. The gun is surrounded by a bucking and focusing solenoids, configured such that they nominally yield a vanishing magnetic field B_{0z} at the photocathode surface. When the solenoids are tuned to provide a

non-vanishing axial magnetic field B_{0z} at the cathode, the electrons acquire a canonical angular momentum (CAM); see Eq. (1). The conservation of the CAM L yields that the mechanical angular momentum (MAM) of the beam in the magnetic-field-free zone is:

$$|\mathbf{L}| = \gamma m |\mathbf{r} \times \frac{d\mathbf{r}}{dt}| = \frac{1}{2} e B_{0z} r_0^2, \quad (2)$$

where is the field at the cathode surface, r_0 is the particle coordinate at the cathode and r is the particle coordinate at the measurement location downstream of the cathode. The norm of $|\mathbf{L}|$ can be computed as $L = |\mathbf{r} \times \mathbf{p}| = x p_y - y p_x$. The particle’s total momentum $\vec{p} = p_r \hat{\mathbf{r}} + p_\theta \hat{\boldsymbol{\theta}} + p_z \hat{\mathbf{z}}$ has non-zero $\hat{\boldsymbol{\theta}}$ -component $p_\theta = \gamma m_e r \dot{\theta}$ resulting in CAM-dominated beam. The associated beam dynamics can be treated via envelope equation formalism, which in the case of magnetized beam takes form [3, 4]:

$$\sigma'' + k_l^2 \sigma - \frac{K}{4\sigma} - \frac{\epsilon_u^2}{\sigma^3} - \frac{\mathcal{L}^2}{\sigma^3} = 0, \quad (3)$$

where $k_l = e B_z(z)/2\gamma m c$ is Larmor wavenumber, $K = 2I/I_0\gamma^3$ is the perveance, I and I_0 are the beam and Alfvén current respectively, ϵ_u - geometric emittance and magnetization $\mathcal{L} \equiv \langle L \rangle / 2\gamma m c$. Magnetized state is achieved when $\mathcal{L} \gg \epsilon_u$.

Since the last two terms in Eq. (3) can be combined, magnetized beams are characterized by eigen-emittance concept, where eigen-emittances are the eigen values of 4×4 transverse beam matrix Σ , and 4D emittance is $\epsilon_{4D} \equiv \gamma |\Sigma|^{1/4}$.

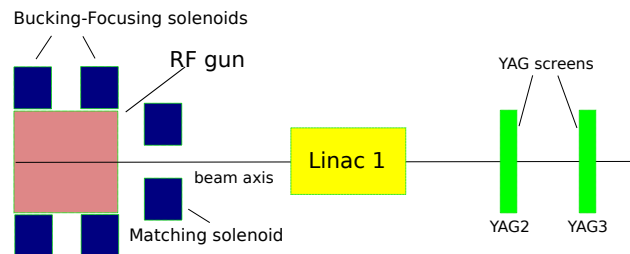


Figure 1: Overview of the AWA witness beamline. The overlap of two solenoid fields produces CAM-dominated beams.

* This work was supported by the US Department of Energy under contract No. DE-SC0011831 with Northern Illinois University. The work by the AWA group is funded through the U.S. Department of Energy, Office of Science, under contract No. DE-AC02-06CH11357.

The eigenvalues ϵ_{\pm} of Σ can be found as [5, 6]:

$$\det(J\Sigma - i\epsilon_{\pm}I) = 0, \quad (4)$$

where I and J are respectively unit and symplectic unit matrices. A detailed eigen-emittance study of a magnetized beam was performed in [7].

METHOD TO MEASURE \mathcal{L}

An electron beam consisting of multiple beamlets projected on a photocathode immersed into magnetic field will shear due to the kinetic angular momentum. Therefore a measurement of the rotation angle provides an indirect measurement of mechanical angular momentum; see Fig. 2. A similar method was discussed in Ref. [8] for the case of slits located downstream of the electron source.

We validate the proposed method via numerical simulations with the program IMPACT-T [9] and consider the AWA witness beamline diagrammed in Fig. 1. A code that converts laser spot picture into a particle distribution was developed in a similar fashion with [1, 10]. In this approach the image is being randomly accessed and the value at a given point is used as a probability of seeding the particle. The longitudinal component and thermal emittance are calculated in ASTRA generator program [11]. The resulting particle distribution is then converted into IMPACT-T format and tracked through the beamline.

The particle distribution is saved at two locations of YAG screens (YAG2 and YAG3 in Fig. 1) and away from the waist; the centroids $(x_{i,j}^{(k)}, y_{i,j}^{(k)})$ of the (i, j) beamlet at YAG(k) is found (where $k = 2, 3$). The MAM associated to the (i, j) beamlet can then be inferred as $L_{i,j} \equiv c[x_{i,j}^{(1)}(y_{i,j}^{(2)} - y_{i,j}^{(1)}) - y_{i,j}^{(1)}(x_{i,j}^{(2)} - x_{i,j}^{(1)})]/d$ where d is the distance between the YAG viewers. The magnetization is then deduced by an averaging of $L_{i,j}$ over the beamlet array. Likewise the standard deviation of $L_{i,j}$ provides an errorbar on the measurement. To validate the technique, we performed

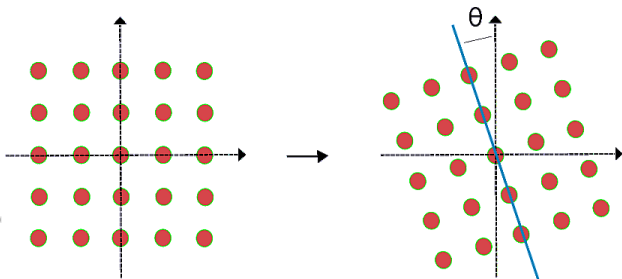


Figure 2: The relative shearing of the beamlet formation due to electron beam magnetization (sketch).

numerical simulations for different B_{0z} field values and results are summarized in Fig. 3. The latter Figure confirms that the CAM (as inferred from the value of B_{0z}) is fully transferred to the MAM. Some systematic discrepancies ($< 5\%$) are observed as \mathcal{L} increases and they are most likely due to the contribution of nonlinear terms in multipole expansion of $B(z)$ not accounted for in Eq. (3) (which assumes

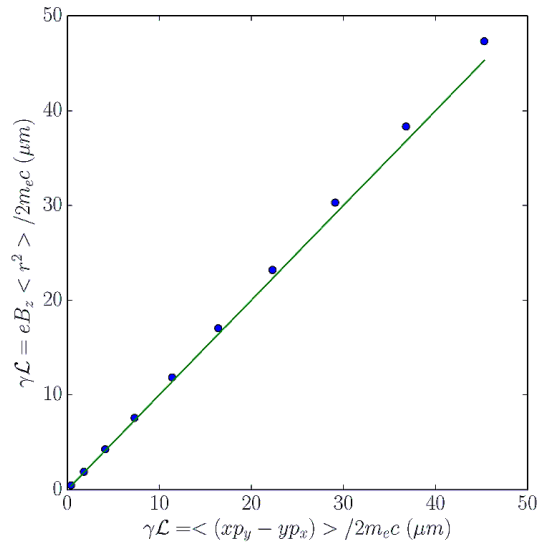


Figure 3: Proof-of-principle via numerical simulations in IMPACT-T of the measurement method. Magnetization \mathcal{L} is computed from the particle distribution (blue markers) as function of magnetization computed from known B_{0z} (green solid line).

a paraxial linear approximation). Likewise space-charge effects might alter the results. Both limitations will be the object of further studies.

Nevertheless, the simulations demonstrate that using a patterned laser beam to trigger emission provides a simple method to measure the MAM. Additionally, this method may serve as a beam-based diagnostic tool to investigate the impact of B-field nonlinearities at the cathode and space charge.

In case when the bucking solenoid has the opposite polarity with the focusing solenoid (normal operation), the magnetization of the beam will be due to the residual B-field of the focusing solenoid when the bucking solenoid current is decreased, and therefore will not be large. In this case, one can still perform the measurement using the described technique by comparing the beamlet pattern to the reference setting where the $B_{0z} = 0$. In such a case, one can rely on using a single YAG viewer, but the measurement will not provide the absolute value of B_{0z} . However, since it leverages on the longer arm of the beamline, the beamlets have enough time to shear when the value of p_{θ} is small. This has fundamental systematic error due to the assumption the beam is relativistic after the gun and the gun size is much shorter than the position of the YAG screen. However, it is a reasonable assumption for sake of simplicity of the presented method.

Due to the complicated beam dynamics of each beamlet, in case of same polarity of bucking and focusing solenoids, the measurement of the relative rotation between two YAG screens provides more accurate value of B_{0z} , since the value of p_{θ} becomes relatively large.

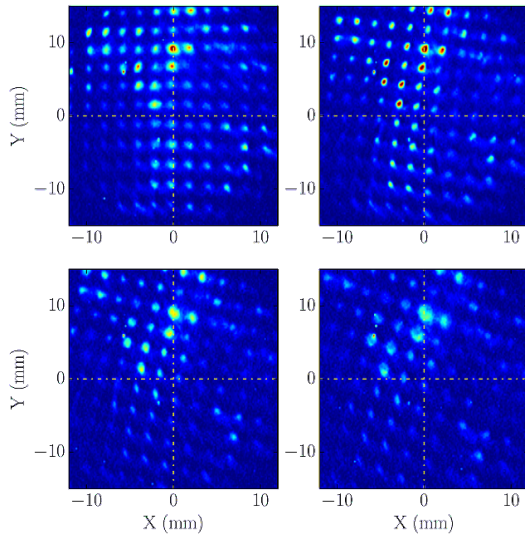


Figure 4: Beamlet formation for (top-right to bottom-left) $B_{0z}=0, 180, 300, 460$ Gauss residual field at the cathode observed at YAG2 location. The yellow dashed lines are drawn for reference.

E-BEAM EXPERIMENT

A preliminary experiment was performed at the AWA “witness” beamline. A 12×12 laser beamlet pattern with rms duration of 6 ps was formed by using the microlens-array technique detailed in Ref. [1]. The ~ 5 -MeV beam out of the RF gun was further accelerated using the L-band linac to ~ 10 MeV; see Fig. 1. As the total laser intensity is distributed among the beamlets, the charge per beamlet can be made very small to mitigate space charge effects. When the threshold of a typical OTR(YAG) is reached (several fC) [12], the number of electrons per beamlet is close to the number of electrons per macroparticle, which provides a direct comparison between experiment and simulations. This extends the application of the patterned beam to experimentally probe nonlinear effects where each beamlet acts as a “macroparticle”. In the experiment, the total charge was 60 pC per bunch, resulting in ~ 420 fC per beamlet.

The three solenoids depicted in Fig. 1 were controlled independently via unipolar power supplies. We started with the normal operational configuration where the bucking and focusing solenoids had opposite polarities which yielded to relatively low magnetization of the beam, and we consequently proceeded with the technique based on using one YAG viewer. The YAG2 viewer, located at 2.79-m from the cathode, was used; see Fig. 1. The bucking solenoid current was slowly decreased to 0 A and the induced rotation of the beamlet formation was observed; see Fig. 4.

This technique provides excellent determination of the magnetic axis and probes the laser spot alignment. After the center of rotation was found, the MAM of each beamlet was recovered via Eq. (2), providing statistical error bars of the

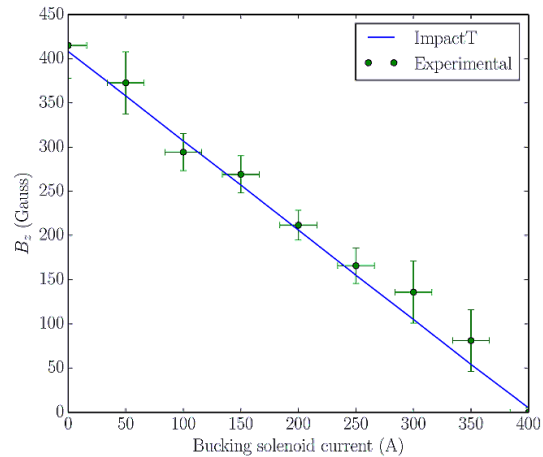


Figure 5: Comparison between IMPACT-T simulations and experimentally recovered values of B_{0z} from image shown in Fig. 4.

measurement. Due to non-ideal beam alignment, charge and solenoid current fluctuations, the rms error of the recovered B_{0z} is ± 42.5 Gauss; see Fig. 5.

Additional improvements of the technique and data analysis will be made in subsequent experiments planned at AWA facility in the near future.

SUMMARY

We demonstrated numerically and experimentally a simple method for measuring electron beam magnetization via laser beamlet rotation technique. Microlens array laser shaping was used to produce beamlets at the photocathode at AWA facility. The values of B_{0z} field were reconstructed for several bucking solenoid currents, proving the usability of the technique. Besides measuring the magnetization, patterned beams may serve as a diagnostic tool for magnetic field and accelerator nonlinearities studies. Further experiments at AWA facility are planned in the near future.

REFERENCES

- [1] A. Halavanau *et al*, FERMILAB-TM-2634-APC (2016).
- [2] R. Brinkmann, Ya. Derbenev, and K. Flottmann, *Phys. Rev. ST Accel. Beams*, **4**, 053501 (2001).
- [3] M. Reiser, "Theory and design of charged particle beams", (1995).
- [4] S. Lidia, LUX Tech Note-012, LBNL-56558 (2012).
- [5] K. Kubo. "How to calculate intrinsic emittances from 4-dimensional beam matrix", ATF Internal Report, ATF-99-02 (1999).
- [6] P. Piot and Y. E. Sun. "Generation and Dynamics of Magnetized Electron Beams for High-Energy Electron Cooling", FERMILAB-CONF-14-142-APC (2014).
- [7] J. Zhu, P. Piot, D. Mihalcea, and C. R. Prokop, "Formation of Compressed Flat Electron Beams with High Transverse-Emittance Ratios", *Phys. Rev. ST Accel. Beams*, **17**, 084401 (2014).

- [8] Y. E. Sun, P. Piot, K. J. Kim, N. Barov, S. Lidia, J. Santucci, R. Tikhoplav, and J. Wennerberg. "Generation of angular-momentum-dominated electron beams from a photoinjector", *Phys. Rev. ST Accel. Beams*, **7**, 123501 (2004).
- [9] J. Qiang, *IMPACT-T reference manual*, LBNL-62326, (2007).
- [10] M. Rihaoui, P. Piot, J. G. Power, Z. Yusof, and W. Gai. "Observation and simulation of space-charge effects in a radio-frequency photoinjector using a transverse multibeamlet distribution", *Phys. Rev. ST Accel. Beams*, **12**, 124201 (2009).
- [11] K. Flöttmann, *ASTRA reference manual*, DESY (2000).
- [12] J. Power, Private communication (2016).